Int. J. Heat Mass Transfer. Vol. 34, No. 1, pp. 253–266, 1991
Printed in Great Britain

0017–9310/91 $3.00+0.00

Solution of the inverse radiation problem for inhomogeneous and anisotropically scattering media using a Monte Carlo technique

SHANKER SUBRAMANIAM and M. PINAR MENGÜÇ
Department of Mechanical Engineering, University of Kentucky, Lexington, KY 40506, U.S.A.

(*Received* 7 *August* 1989 *and in final form* 6 *March* 1990)

Abstract—An analysis is presented for the solution of the inverse radiation problem using a Monte Carlo technique. For inhomogeneous planar media, the profile of the single scattering albedo is obtained from the inverse analysis. For homogeneous, anisotropically scattering media, the single scattering albedo and the asymmetry factor are recovered. A step phase function approximation is used to account for the anisotropic scattering in the medium. The confidence bounds on the estimated parameters for errors in the input data are evaluated. The results show that the medium properties can be recovered with high accuracy even if there is up to 10% error in the input data. The primary advantage of the Monte Carlo method is that a single direct solution yields the coefficients of a multivariate polynomial for each set of observation data, which are then used to obtain the medium properties by a non-linear least-square minimization technique.

INTRODUCTION

RADIATION is the predominant mode of heat transfer in high temperature applications such as industrial furnaces, boilers, gas turbine combustors, as well as in fires. The distribution of radiative heat flux and its divergence are required for thermal modeling of these systems. They are obtained from the solution of the radiative transfer equation (RTE) for a given geometry, set of boundary conditions and radiative properties of the combustion products, i.e. particles and gases [1].

Radiative properties of particles can be theoretically determined using physical input parameters such as the wavelength of the incident radiation, the complex refractive index, the shape, size, and volume fraction distribution of the particles in the system. The shape of the particles is usually irregular and random; therefore, it is necessary to assume an average, smooth shape, such as a sphere, to determine particle properties theoretically. The complex index of refraction, on the other hand, is a function of the wavelength of the incident radiation and physical and chemical properties of the material. It cannot be measured directly and it is required only to theoretically determine the radiative properties of particles. For these reasons, it is preferable to determine the relevant radiative properties from experiments *in situ*. This can be accomplished by combining optical diagnostic techniques with inverse analyses of the radiative transfer problem. Here only one set of experimental errors will be involved, and the properties so obtained will be particular to the system under consideration. Our goal in this study is to develop a versatile technique for inverse radiation analyses in planar systems.

The radiative transfer equation

The RTE considered in this work is for azimuthally symmetric plane parallel media and is written as [2, 3]

$$\mu\frac{\partial}{\partial\tau}I(\tau,\mu)+I(\tau,\mu)=\frac{\omega(\tau)}{2}\sum_{l=0}^{L}a_lP_l(\mu)\times\int_{-1}^{1}P_l(\mu')I(\tau,\mu')\,\mathrm{d}\mu'. \quad (1)$$

The boundary conditions required for the direct and inverse solution are the incident intensity distributions at the two faces of the plane parallel medium. For all of the cases considered here, the boundaries are assumed nonreflecting, with $I(0,\mu)=1$ and $I(\tau_0,-\mu)=0$ for $0\leqslant\mu\leqslant1$. Definitions of all the parameters used are given in the Nomenclature. It should be noted that all radiative properties are wavelength dependent, although this dependency is not shown explicitly in the relations.

The RTE, equation (1), is solved to obtain the radiation intensity distribution in the medium. Although several techniques are available for the solution of the RTE [1–6], there is no universally accepted RTE model which can be used for all types of problems. Among all these models, the statistical Monte Carlo technique appears to be the most versatile approach. With increasing availability of high-speed computers, this technique is expected to gain even more recognition [1, 6].

NOMENCLATURE

a_l	coefficients of the phase function expansion
A	minimization quantities
e	error vector
E	mathematical expectation
f	probability density function, PDF
F	cumulative probability distribution function, CDF
g	asymmetry factor
h	step function peak
H	Heaviside or step function
I	radiation intensities
J	number of scatters scored per history
K	number of observations
L	number of coefficients of the phase function expansion
M	number of inverted parameters
n	number of scatters used in computations
N	number of histories
P	probability
Q	fluxes
r	minimization weight factor
s	exponential constant
W	Monte Carlo weights
y	physical distance.

Greek symbols

α	error estimates
β	extinction coefficient
γ	discrete central value
δ	Dirac-delta function
θ	polar angle
Θ	angle between incident and scattered radiation
κ	inversion parameter
λ	wavelength
μ	polar direction cosine
ν	maximum number of scatters before escape
ξ	pseudo-random number
σ	standard deviation
τ	optical thickness
υ	scattered direction cosine
Υ	biasing probability fraction
ϕ	azimuthal angle
φ	azimuthal angle
Φ	scattering phase function
ω	single scattering albedo
Ω	solid angle of propagation.

Subscripts

b	biasing
c	minimization
d	detector
f	last flight estimation
i, j, k	summation or array index
s	sampling
t	total
x	importance.

Superscripts

$\hat{}$	computed statistical estimate
$\tilde{}$	averaged statistical estimate
$\bar{}$	correct statistical estimate
$\ddot{}$	quantities with experimental error
$'$	incident direction
$\check{}$	approximated quantity.

In Monte Carlo techniques, a finite number of photons which obey the physical restraints of the RTE are considered. Their initial directions, scattering angles and the distances between each consecutive scatter are computed using pseudo-random number generators. Since a physical modelling of the RTE is used, this approach can be readily applied to diverse geometries and easily accounts for medium inhomogeneity and anisotropy. However, since it is a statistical estimation technique, the solutions, while converging to the 'exact' results for a large number of statistical samples, will always have some error. It is therefore left to the user's discretion, computational power, and felicity to obtain the desired accuracy. This method has long been used in the solution of radiative transfer [2, 5] and neutron transport problems [5, 7]. A more complete review of Monte Carlo methods and the various error reduction techniques used therein are given in refs. [5, 8, 9].

Whereas in a direct solution of the RTE, the medium properties and the boundary conditions are used to obtain the radiation intensities and fluxes within and leaving the medium, in the inverse problem one or more of the medium properties are determined using the measured exit fluxes and intensities. Earlier investigators have considered inverse radiation problems where isotropic radiation is incident on plane parallel, homogeneous, isotropically scattering [10–12], as well as anisotropically scattering [13–24] media. Only a few investigators have considered inhomogeneities in the medium [25, 26]. In another group of inverse problems, measurements within the medium have been employed to obtain the similarity parameter, which combines the asymmetry factor and the single scattering albedo into one unknown [27–30]. Reviews of these inverse solution techniques are available in the literature [31–33].

Inverse problems other than simple one-dimensional systems have not received much attention in the past and only a few studies have appeared in the

literature [34–36]. The main reason for this is two-fold: first, there is a lack of efficient direct solution methods for multidimensional, inhomogeneous, and anisotropically scattering media, which yield accurate radiative intensity distributions and can be employed in iterative or least-square minimization based inversion schemes, and second, it is very difficult to develop inverse solution algorithms for general geometries which do not require the solution of the direct problem. Monte Carlo techniques appear to be the only viable approach to solve the direct and inverse radiation problem in complicated geometries.

In this paper, we introduce a Monte Carlo solution technique for the inverse radiation problem for inhomogeneous and anisotropically scattering planar media. A functional form of the single scattering albedo is considered for inhomogeneous media. For the case of anisotropic scattering, a new step phase function approximation is employed to evaluate the asymmetry factor of a homogeneous, anisotropically scattering system.

It is worth noting that here we will assume the medium optical thickness is known. Therefore, the technique, as presented here, can only be used for the solution of a practical problem, if the optical path length is measured from independent experiments. However, it may be possible to use this methodology in an iterative algorithm to predict the optical thickness; this will be considered in a separate study.

MONTE CARLO SIMULATION

A detailed outline of the developed Monte Carlo method of solution for the direct and inverse problems is described in refs. [37, 38]. Here, we will present only a summary of the method. First, we will explain the statistical sampling procedures. Then the direct and inverse solution of the radiation problem with the importance sampling technique will be discussed.

Statistical sampling

Monte Carlo simulation involves the random sampling of the independent parameters of equation (1), i.e. the incident and scattering angles μ and μ', and the scattering distances y or τ, using the corresponding probability density functions (PDFs). If we define $P\{a \leqslant \xi \leqslant b\}$ as the probability that ξ takes a value between a and b, then the PDF is defined as that function $f(\xi)$ which yields the probability of ξ taking a value between ξ and $\xi+\Delta\xi$ as $f(\xi)\Delta\xi$ in the limit as $\Delta\xi \to 0$. Then

$$P\{a \leqslant \xi \leqslant b\} = \int_a^b f(\xi)\,\mathrm{d}\xi. \tag{2}$$

A cumulative probability distribution function (CDF) $F(x)$ yields the probability $P\{\xi \leqslant x\}$, and is defined as

$$F(x) = \int_{-\infty}^{x} f(\xi)\,\mathrm{d}\xi. \tag{3}$$

A uniformly distributed random variable is one the PDF of which is such that the probability of ξ taking a value between ξ and $\xi+\mathrm{d}\xi$ is $\mathrm{d}\xi$. Using pseudo-random number generators, we usually obtain a uniformly distributed random variable ξ between 0 and 1. We can use the CDF to generate x, the random variable that we wish to sample, as $x = F^{-1}(\xi)$.

For obtaining ξ, we can use six different pseudo-random number generation options from IMSL [39], depending on how 'random' we would like ξ to be. Three multipliers are used in this generation; options 1 and 2 use 16 807 as the multiplier, 3 and 4 use 397 204 094, and 5 and 6 use 950 706 376. In addition, options 2, 4, and 6 employ an additional shuffling process which involves generation of a table of 128 random numbers, shuffling them, and selecting randomly from this table. Option 1 was the simplest and computationally the fastest, while option 6 was more 'random' and takes the longest time for generation. In our preliminary computations, we considered all these options; the results reported in this paper were generated using option 1 [37].

Direct Monte Carlo solution

For a given source of photons, the initial direction can be sampled from either the intensity $[F_I(\mu)]$ or the flux $[F_F(\mu)]$ distribution. For each photon history, a sampling weight, $W_s = \mu_0$, is used for every score for the fluxes when sampling from a unit intensity distribution, and $W_s = 1/2$ when sampling from a unit flux density distribution. The history weight is the product of the initial sampling weight W_s and scattering probability ω (i.e. the single scattering albedo) at every scatter. Here, a history is defined as one complete random sequence which yields an estimate for the statistical quantities to be evaluated, and a run comprises of N such histories.

The probability of the photon penetrating to a distance y is $\mathrm{e}^{-\beta y}$, where β is the extinction coefficient and y the physical distance travelled by the photon. This yields the CDF for the scattering distance as $F(y) = 1-\mathrm{e}^{-\beta y} = \xi$, from which the collision distance y is evaluated as $y = -\ln \xi/\beta$. Thus, we must know β, the extinction coefficient, to perform the direct Monte Carlo simulation. In the analysis presented here, we assume β is known.

Ordinarily, scoring for the exit fluxes is done when the photon exits the medium. It is preferable to score for all photons scattered in the medium to reduce variance in the results, since there will be more scores for each history. This can be accomplished by stretching each flight path and simulating escape before each scatter. This is called last flight estimation (LFE). The probability of such an escape is

$$W_f = \begin{cases} \mathrm{e}^{-(\tau_0-\tau_i)/\mu_i} & \text{if } \mu_i > 0 \\ \mathrm{e}^{\tau_i/\mu_i} & \text{if } \mu_i < 0 \end{cases} \tag{4}$$

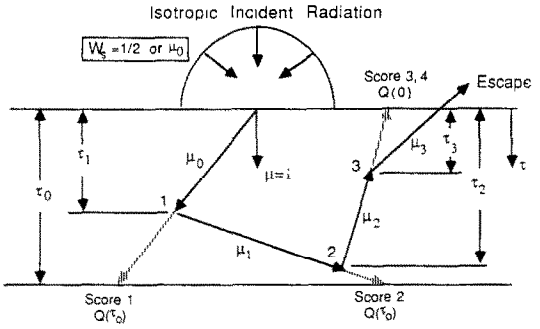

FIG. 1. The last flight estimation for a photon with three scatters before escape. LFE extensions shown as the dashed lines.

for the ith scatter. Here W_f is denoted as the LFE weight. In Fig. 1, we show these extensions before each scatter by the dashed lines, and indicate the LFE distances τ_i and direction cosines μ_i [37].

For scattered intensities, a LFE weight W_f similar to equation (4) is obtained by replacing μ_i with μ_d, the direction cosine of the detector angle. The intensities are scored by the product of the history weight W_s and W_f. Here $W_s = \mu_0/2\mu_d$ when sampling from the unit intensity distribution and $1/4\mu_d$ when sampling from the unit flux distribution. Also, the direct transmitted intensity $e^{-\tau_0/\mu_d}$ should be included in the weight for the entire direct run (not for each history). At each scatter point, the cumulative history weight is further multiplied by ω, the single scattering albedo, which may be a function of the optical thickness.

The photon direction after interaction is sampled next, for which the CDF is written as

$$F(\theta) = \left[\int_0^{\theta} \Phi(\cos\theta')\sin\theta'\,d\theta'\right] \Big/ \left[\int_0^{\pi} \Phi(\cos\theta')\sin\theta'\,d\theta'\right] \quad (5)$$

where $\Phi(\cos\theta')$ is the Legendre polynomial expansion of the scattering phase function as in equation (1). For isotropic scattering, $\Phi(\cos\theta') = 1$ and this yields $F(\theta) = (1-\cos\theta)/2 = \xi$ which is used to compute $\mu(=\cos\theta)$, after ξ is obtained from a random number generator. Using this value of μ, the backscattered or transmitted flux densities are scored using the LFE, and the optical distance to the next scatter point is computed. If this point lies outside the medium, the history is terminated without any further scoring. Otherwise, the intensities are scored, the next scatter angle is sampled, and the history continued until the photon escapes, or until the maximum number of scatters is reached. For purposes of computation, we limit the total numbers of scatters for each history to n.

Inverse Monte Carlo solution

Inverse solution techniques, such as those given in refs. [11, 12, 16, 21, 23–26], involve iterative convergence using several direct solutions of the radiative transfer equation. The iterations are terminated when the direct solution results using the 'converged' property values are acceptably close to the 'measured' intensity or flux values. However, using a Monte Carlo technique with the concept of importance sampling requires only a single direct Monte Carlo simulation. Using importance sampling, the unknown probability density function (PDF) is replaced by a known PDF during the simulation, and the unknown PDF appears as a multiplicative weighting function which is to be evaluated.

Historically, the concept of importance sampling arose from the need to reduce the statistical uncertainty in the direct Monte Carlo estimates [5, 8]. The name stems from the fact that, in order to reduce the variance, the random sampling should yield more samples from the more important parts of the sampling region [5, 37]. The use of this concept offers the primary advantage of the inverse Monte Carlo method over other inverse methods that use iterative convergence, such as those developed in refs. [12, 24, 26], because the unknown parameters are not used in the direct solution.

For the case of isotropic scattering, an estimate for the backscattered and transmitted fluxes can be obtained of the form

$$\left.\begin{aligned}\hat{Q}(0) &= \int_0^1 I(0,-\mu)\mu\,d\mu \Big/ \int_0^1 I(0,\mu)\mu\,d\mu \\ \hat{Q}(\tau_0) &= \int_0^1 I(\tau_0,\mu)\mu\,d\mu \Big/ \int_0^1 I(0,\mu)\mu\,d\mu\end{aligned}\right\} = \frac{1}{N}\sum_{i=1}^{N} W_i \quad (6)$$

where N is the total number of histories (or incident photons) and W_i the total increment of the scored quantities for each history given as

$$W_i = W_s \sum_{j=1}^{J_i} W_{f,j}\omega_0^{\nu_j}. \quad (7)$$

Here, the quantities within the summation sign are the LFE weights, and J_i a variable number. When scoring for the fluxes, $J_{i,0}$ is the number of scatters in the ith history where the scattered angle $\mu_j < 0$, and $J_{i,1}$ is the number of scatters in the ith history where the scattered angle $\mu_j > 0$. When scoring for the intensities $J_i = N$. Also, τ_j is the optical depth at which the jth scatter occurs, and ν_j the actual total number of scatters for each value of j.

A similar equation for the case of constant single scatter albedo was given by Dunn [11], where he assumed that the total number of scatters, n, is the same as the total interactions with scattering in either direction, J_i, for every source photon. While this is true when scoring for the intensities, it is not correct when scoring for the fluxes, since $J_{i,0}+J_{i,1} \leqslant n$. Scoring for the intensities can also be performed during the direct simulation using this concept, with the

fluxes replaced by the intensities in equation (6) and using the corresponding weights W_s and W_f for the particular angle of interest.

For equation (6), and knowing W_s and W_f in equation (7), we obtain an estimate for the backscattered and transmitted fluxes of the form

$$\hat{Q}(0) = b_1\omega_0 + b_2\omega_0^2 + b_3\omega_0^3 + \cdots + b_v\omega_0^v, \quad v \leqslant n$$

$$\hat{Q}(\tau_0) = b_0 + b_1\omega_0 + b_2\omega_0^2 + b_3\omega_0^3 + \cdots + b_v\omega_0^v, \quad v \leqslant n \tag{8}$$

where v is the maximum number of scatters before escape. Note that the b-coefficients of $\hat{Q}(0)$ and $\hat{Q}(\tau_0)$ in equation (8) are not the same. Because these coefficients are determined following the same procedures, we preferred to refer to them with a single parameter to facilitate the discussion in the rest of the paper. These polynomials have all coefficients positive, which means that their value is monotonically increasing with ω. Therefore, there is only one single positive root which will satisfy equation (8) and it is found by either a simple iterative procedure, or using non-linear regression routines [39].

The coefficients b_i in equation (8) can be used with several sets of experimental observations for the same set of unknowns, without having to solve the direct problem again. Also, if the value of the sampling parameters such as τ_0, W_s, are the same, the coefficients b_i can be used with the observed values of fluxes for different media with different, but constant, ω. Thus one direct run of the Monte Carlo method can be used repeatedly for several inverse solutions.

The least squares minimization routines minimize the quantity

$$E^2 = \frac{1}{2}\sum_{k=1}^{K}\left\{\frac{\hat{A}_k - A_k}{W_{c,k}}\right\}^2. \tag{9}$$

Here A_k is either the flux (see equation (8)) or intensity value input, $\hat{A}_k$ its direct estimate using the current values of the unknowns, K the total number of observations of fluxes and intensities, and $W_{c,k}$ the minimization weights to account for the magnitudes of the different observations A_k, usually set as

$$W_{c,k} = A_k^r \tag{10}$$

where r is some fraction. Unless otherwise mentioned, we set $r = 0$, which yields $W_{c,k} = 1$ for all the observations. This choice results in a minimization of the differences, which is preferable when we would like to ignore the effect of possibly larger percentage errors in the intensities/fluxes of smaller magnitude. For cases where importance is to be given to all observations, however small they may be, $r = 0.25$ or 0.5 yields more efficient convergence.

The Levenberg–Marquardt algorithm was used in the least squares minimization routine [39]. In this minimization technique, a trust region approach was employed, as discussed by Dennis and Schnabel [40], which yields an increment for the unknown variables during each iteration. This increment is given as

$$\Delta\hat{\Lambda}_i = [R^t R + \rho[1]]^{-1} R^t e \tag{11}$$

where R is the Jacobian containing the partial derivatives of the minimization quantity for each observation with respect to the vector of variables, ρ the Levenberg–Marquardt parameter, [1] the identity matrix, $\Delta\hat{\Lambda}_i$ the column vector of the increments to the vector of variables $\hat{\Lambda}$ for the ith iteration, and e the column vector of the current minimization quantity for each observation as given in equation (9) without squaring, namely

$$e_k = (\hat{A}_{i,k} - A_k)/W_{c,k}. \tag{12}$$

With $\rho = 0$ and e as the vector of the differences between the final direct estimates and the observed values, equation (11) yields the vector of errors in the inverted quantities. In the bounded least squares approach to evaluate the values of the variable within specified bounds, an additional active set strategy proposed by Gill and Murray [41] was employed.

The details of the variance and confidence bounds we consider here are discussed in refs. [37, 38], and they are similar to those given in refs. [12, 26]. The only difference is that, in addition to the errors in the measured quantities $\ddot{A}$, which are the observed values to be used in the inverse method, we will have the standard deviation of the direct Monte Carlo simulation. Then, the total standard deviation of $\ddot{A}$ to be used to compute the standard deviation for the inverse solution can be written as

$$\sigma_t(\ddot{A}) = [\sigma^2(\hat{A}) + \sigma_{exp}^2(\ddot{A})]^{1/2}. \tag{13}$$

A direct analytical solution is performed to eliminate $\sigma(\hat{A})$ in equation (13). Here only the experimental errors contribute to the inverse solution, as in the inverse solutions of Ho and Özişik [12, 26]. In a Monte Carlo simulation, however, the $\sigma(\hat{A})$ contribution could be significant.

The upper bounds for the errors can be evaluated approximately by using the similarity of equation (11) to linear models theory [42], as

$$[\sigma^2(\hat{\Lambda})] = \sigma^2(\tilde{A}) \cdot \mathrm{diag}\,[R^t(\hat{\Lambda})R(\hat{\Lambda})]^{-1} \tag{14}$$

where $\sigma(\tilde{A})$ is a scalar quantity which we set as the maximum value of the errors in the observations, and $\hat{\Lambda}$ the vector of inverse estimates, as in equation (11).

ISOTROPICALLY SCATTERING INHOMOGENEOUS MEDIA

The details of the analysis for determining the single scattering albedo in plane parallel, isotropically scattering media are discussed in ref. [37] for a single homogeneous layer, inhomogeneous half space, and two homogeneous layers. Since these are similar to the problems solved by Dunn [11, 25], we will not

discuss them here. Instead, we will focus on a single inhomogeneous layer with exponential varying single scattering albedo. The exact solution of this problem with the F_N method is given in ref. [43] for both isotropic and collimated incident flux boundary conditions.

The slab single scattering albedo is assumed to have a functional form as $\omega_0 e^{-\tau/s}$, where τ is the optical thickness and ω_0 and s are constants to be evaluated in the inverse problem ($M = 2$). As the value of s increases, the slab approaches a homogeneous single layer. Dunn [25] solved this problem assuming the slab to be composed of five layers with constant albedo in each layer. He considered the case where the total optical thickness τ_0 is 5, and $s = 1$, $\omega_0 = 1$.

First, we attempted to simulate the results reported by Dunn [25]. The discrete values of the single scattering albedo were used in each of the five discrete layers as given in ref. [25] to obtain the Monte Carlo direct estimates for the exit fluxes and intensities. These results were compared against those of the F_0 method. The backscattered flux and intensity values obtained this way were different in the second significant digit, whereas the transmitted flux values differed in the first digit. To ensure that we did not make any error in calculation, we also obtained the discrete ordinate results [44] for the five layer approximation using the albedo values given in ref. [25]. These results were in very close agreement with our direct Monte Carlo results, but not with the input F_N results used by Dunn [25] to obtain the ω profile from inverse calculations. This suggests that there may be a numerical error in the inverse results given in ref. [25]. Using our Monte Carlo technique and the F_N results, we obtained the discrete values of ω as 0.778, 0.001, 0.001, 0.001, 0.087, whereas Dunn reported values of 0.74, 0.27, 0.10, 0.037, 0.014. The bounds used in our calculations were $0.001 \leqslant \omega \leqslant 1.0$, and we used the two fluxes and three intensity values for inversion.

We also tried other methods of obtaining the variation of the albedo. First, we used an exponential function for ω. By taking $\kappa = e^{-1/s}$, we scored with $\omega_0 \kappa^{\tau}$ for every scatter using importance sampling. We then obtained an expression in the unknowns ω_0 and κ, which we solved using a least squares technique. Since τ appeared in the exponent and an infinite number of τ values were possible in sampling, it was necessary to discretize the possible values to a finite number.

For the vth scatter, the importance sampling weight is

$$W_p = \omega_0^v \prod_{i=1}^{v} \kappa^{\tau_i} \tag{15}$$

where $0 \leqslant \tau_i \leqslant \tau_0$ to be different in each history. If we restrict the direct simulation to n scatters, the maximum value of the exponent will be $n\tau_0$. We divided this maximum into nt discrete divisions, each of which had a central value γ_l. Then, using equations (6), (8), and (15), we obtained the following equations:

$$\hat{A}_k = \sum_{v=0}^{n} \sum_{l=1}^{nt} b_{vl}, \quad k = 1, 2, \ldots, K \tag{16}$$

where

$$b_{vl} = \frac{W_s}{N} \omega_0^v \kappa^{\gamma_l} \sum_{j=1}^{J} W_{f,j}. \tag{17}$$

The observations used were $Q(0)$, $Q(1)$, $I(\tau_0, 0.5)$, $I(0, -0.5)$, and $I(0, -1)$. Therefore, the total number of observations, K, was 5. Here J is the number of histories where, for the vth scatter, $\sum_{i=1}^{v} \tau_i$ is within the corresponding discretized element of which γ_l is the central value, and μ_v is in the corresponding exit direction when scoring for the fluxes. When scoring for intensities, $J = N$, since scoring is done at every scatter. Again, values of W_f are the last flight estimation weights.

After obtaining the coefficients b_{vl} of equation (8) for the five observations, we used bounded and unbounded least squares procedures [39] to obtain the values of ω_0 and κ. For this case, we used a value of $r = 0.25$ in equation (10) for the minimization weights, to have convergence with fewer iterations. The errors in the inverted quantities, calculated using equation (11) with $\rho = 0$, were always seen to be in agreement with the actual errors. The results of these computations are given in Table 1. For cases II and III, the vector e used in equation (11) was obtained from the error in the observations only and yielded the change from the converged results of case I.

In experimental observations, it is probable that the readings of smaller magnitude have greater scope for error. With this in mind, we considered random errors within ± 2, 10, 20, 2, 2% respectively, for the five observations and performed inverse runs with 20 such sets of errors, with $r = 0.25$ (see Fig. 2). In order to calculate the upper bounds, we took $\sigma(\tilde{A})$ as the maximum value in the vector e. Using this, we calculated the bounds as ± 0.123 and ± 0.149 for $\hat{\omega}_0$ and $\hat{\kappa}$, respectively. With $r = 0$, these bounds were ± 0.137 and ± 0.168. Figure 2 shows that the converged results are well within the predicted bounds and the maximum value of ω_0 corresponds to the minimum value of κ, and vice versa. Two single scattering albedo profiles based on these converged results (worst cases) are plotted against the exact functional expression for ω in Fig. 3. The agreement between the exact and recovered profiles is satisfactory.

We also considered the case of collimated radiation incident on one boundary at other than the normal direction. All the medium properties were the same as for the case of isotropic incidence, and the F_N direct results were obtained from ref. [43]. The only difference in the direct method was that the incident direction cosine $\mu_0 = 0.9$ was considered for all the histories. The sampling weights W_s used were μ_0 and $\mu_0/2\mu_d$ for the fluxes and intensities respectively, when sampling for photons with unit flux density normal to the face. We considered random errors the same as

Table 1. Inverse Monte Carlo results. With $\omega = \omega_0 \kappa^{\tau}$ (exact values for $\omega_0 = 1.0$, $\kappa = 0.368$) 40 000 histories and six scatters for the direct simulation

	Unbounded convergence				Bounded†	
Error	$\hat{\omega}_0$	$\hat{\kappa}$	$\hat{\alpha}(\hat{\omega}_0)$	$\alpha(\hat{\kappa})$	$\hat{\omega}_0$	$\hat{\kappa}$
I	1.005	0.372	0.0048	0.0039	1.000	0.379
II	1.017	0.371	0.0126	−0.0010	1.000	0.396
III	1.030	0.370	0.0249	−0.0019	1.000	0.413

I, No experimental error, [e] = exact-direct Monte Carlo.
II, 2% experimental error, [e] = observed-exact.
III, 4% experimental error, [e] = observed-exact.
† The bounds are $0.001 \leqslant \hat{\omega}_0, \hat{\kappa} \leqslant 1.0$.

before, and obtained results very similar to those given in Fig. 2.

It is possible to consider a linear function approximation to the exponentially decaying single scattering albedo $\omega = \omega_0 e^{-\tau/s}$, if $s \simeq 10$ or greater, because then the profile approaches a linear one. Thus, assuming that $\omega = \omega_1 + \omega_2 \tau$, and using importance sampling, we solved the direct problem and found these coefficients from the inverse solution. The equations for the observations are obtained in the form

$$\hat{A}_k = \sum_{i=0}^{v} \sum_{l=0}^{i} b_{il} \tag{18}$$

where

$$\sum_{l=0}^{i} b_{il} = \frac{W_s}{N} \sum_{j=1}^{J} W_{t,j} \prod_{l=0}^{i} (\omega_1 + \omega_2 \tau_l). \tag{19}$$

The direct solution for this case takes considerably longer CPU time since a greater number of scatters ($n = 20$ when $s = 10$ and $n = 40$ when $s = 100$) are needed with the same number of histories, and an additional computational loop is to be performed for each score to account for the product within the summation sign in equation (19). For the case of $s = 10$, with 20 000 scatters, the CPU time required for the direct solution was 145 CPU seconds using the IBM 3090-300 supercomputer at the University of Kentucky. The bounds which were calculated for $\hat{\omega}_1$ and $\hat{\omega}_2$ using the maximum value in e were ± 0.0089, ± 0.0107, respectively. The single scatter albedo profiles obtained from the worst results are compared against the exact functional form for ω in Fig. 4.

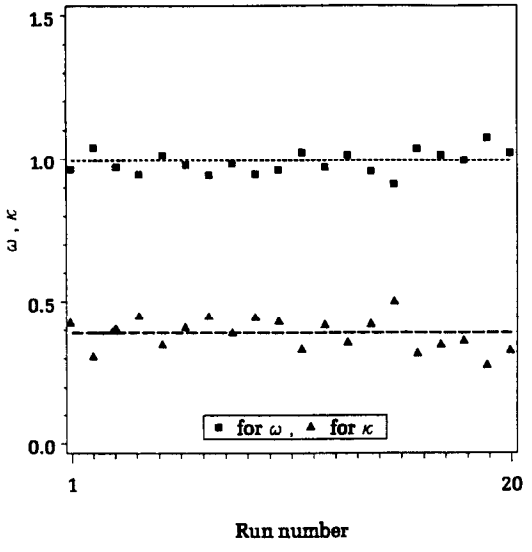

FIG. 2. Inverse results using exponential single scattering albedo profile. Isotropic incident radiation on single inhomogeneous slab. The exact values are $\tau_0 = 5.0$, $\omega_0 = 1.0$, and $\kappa = 0.368$. Converged values without error are $\omega_0 = 1.005$, $\kappa = 0.372$. The upper bounds are ± 0.123 for $\hat{\omega}_0$, and ± 0.149 for $\hat{\kappa}$.

ANISOTROPICALLY SCATTERING MEDIA

In this section, we discuss the inverse problem for anisotropically scattering, plane parallel media. The use of the scattering phase function of order L as in equation (1) in the inverse solution would involve determination of the L a_l coefficients. Therefore, we need an approximation to the phase function that yields acceptably accurate direct results and minimizes the number of unknowns to be evaluated.

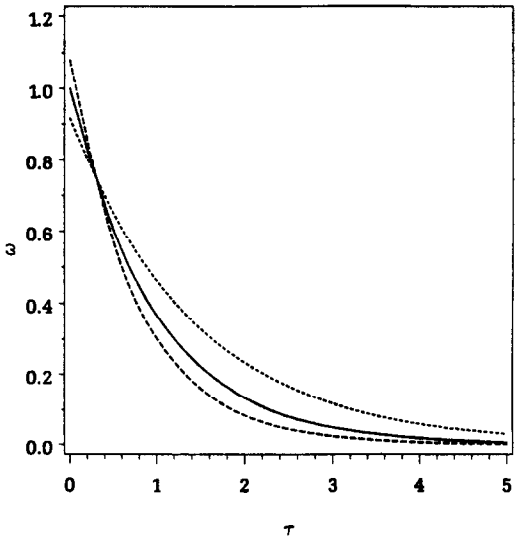

FIG. 3. Comparison of inverse solution results with exact ω-profile. Single layer with $\omega = \omega_0 e^{-\tau/s}$, with $s = 1$. Dashed lines represent the worst inverse solution results.

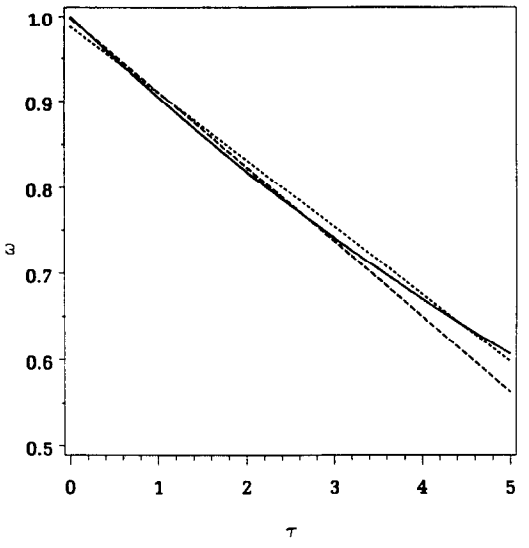

FIG. 4. Comparison of inverse solution results with exact ω-profile. Single layer with $\omega = \omega_0 e^{-\tau/s}$, with $s = 10$. Dashed lines represent the worst inverse solution results.

Phase function approximation and analysis

An indication of the behavior of the scattering phase function for spherical particles can be obtained from the size parameter, x, which is defined as $\pi d/\lambda$, where d is the scattering particle diameter and λ the wavelength of the incident radiation. As the size parameter increases, the particles scatter increasingly in the forward direction, whereas the phase function values in other directions remain, for the most part, within the same order of magnitude. Phase function approximations should be capable of representing such functions with a fewer number of parameters.

In a recent paper [45] a step function approximation for the scattering phase function was outlined, and a solution scheme to recover the first few coefficients of the full phase function from experiments was discussed. This approximation is necessary for the Monte Carlo simulation in order to have a simple form of the phase function which approximates the scattering pattern and yields the same mean cosine of the scattering angle as the original phase function. It is worth noting that Dirac-delta phase function approximations are unsuitable for the Monte Carlo solutions. The delta functions, by definition, possess infinite value at $\Theta = 0$ and cannot be used in any physical sense.

The simplest step phase function approximation is the step-isotropic (SI) phase function, which is written as [45]

$$\check{\Phi}(\mu) = 2hH(\mu-\mu_1)+\{1-h(1-\mu_1)\}. \quad (20)$$

Here $\mu_1 = \cos \Delta\theta_1$, where $\Delta\theta_1$ is the small angle over which the step is defined, and $H(\mu-\mu_1)$ is the step or Heaviside function which has value 1 when $\mu > \mu_1$ and 0 for all other values of μ. The superscript ($\check{}$) is used to denote the approximated phase function or quantity.

As elucidated by Pomraning [46], the best strategy for determining the coefficients of a lower order approximation is to satisfy the lower order moments of the phase function. The phase function given by equation (20) satisfies the zeroth moment. To obtain h, we satisfy the first moment

$$\int \Phi(\mu)\mu \, d\mu$$

which yields

$$h = 2a_1/[3(1-\mu_1^2)] \quad (21)$$

for a given μ_1. Here a_1 is the first coefficient of the full phase function

$$\Phi(\mu) = \sum_{n=0}^{\nu} a_n P_n(\mu) \quad (22)$$

where P_n is the orthogonal Legendre polynomial of order n. The first moment of the phase function yields the mean cosine of the scattering angle or the asymmetry factor, which is also satisfied by the step function approximation.

The step function approximation given by equation (20) yields a reasonable physical approximation to the true phase function. However, when $a_1 > 1.5(1+\mu_1)$, the second term on the right-hand side of equation (20) has a negative value, which is not physically permissible, although the results of the direct simulation may converge to the exact results for larger optical thicknesses and increased number of scatters. In such a case, a larger value of μ_1 is required to ensure that the second term is always positive. This corresponds to a narrower angular step.

The use of the second moment of the phase function yields a step-Eddington (SE) approximation

$$\check{\Phi}(\mu) = 2hH(\mu-\mu_1)+\{1-h(1-\mu_1)\}(1+\check{a}_1\mu) \quad (23)$$

which is a modified linearly anisotropic phase function. Here h and $\check{a}_1$ are given by

$$\check{a}_1 = [a_1-3h(1-\mu_1^2)/2]/[1-h(1-\mu_1)] \quad (24)$$

$$h = 2a_2/[5\mu_1(1-\mu_1^2)]. \quad (25)$$

The results reported in this paper were obtained employing the SI phase function. Written in its azimuthally-dependent form, equation (20) is expressed as

$$\check{\Phi}(\cos\Theta) = 2hH(\cos\Theta-\cos\Delta\Theta_1) + \{1-h(1-\cos\Delta\Theta_1)\} \quad (26)$$

where $\cos\Delta\Theta_1 = \mu_1$, and Θ is the scattering angle in the relation

$$\cos\Theta = \mu\mu'+(1-\mu^2)^{1/2}(1-\mu'^2)^{1/2}\cos(\phi-\phi'). \quad (27)$$

Here μ' and μ are the incident and scattered direction cosines, and ϕ', ϕ are the incident and scattered azi-

muthal angles, all sampled with reference to a fixed coordinate system. For isotropic scattering, we can sample for the azimuthal angle as

$$\phi = \pi(2\xi - 1) \tag{28}$$

in the range $-\pi$ to π [8]. Thus we evaluate cos Θ from equation (27), and multiply the history weight with the probability of scatter, depending on whether cos Θ is smaller or greater than μ_1. This probability is $[1+h(1+\mu_1)]$ for scattering in the step range of the phase function, or $[1-h(1-\mu_1)]$ for the other angles. This quantity, multiplied by ω, will be the importance sampling weight.

In the direct Monte Carlo simulation for the inverse solution, we used the concept of importance sampling to remove the unknowns in the anisotropically scattering phase function. In effect, we sampled for the scattered direction from an isotropically scattering PDF, and weight by the appropriate unknown, depending on whether the scattering is in the step or isotropic portion of the phase function. For $\mu_1 \simeq 1$, this procedure yielded few particles scattered in the forward direction, since we sampled for μ from an isotropic scattering distribution. In order to have a good statistical representation of the forward scattering, we needed to force more particles to scatter in the forward step region, which is called biasing.

The solution of equation (27) for μ, when $\phi = \phi'$ and cos Θ = cos $\Delta\Theta_1 = \mu_1$, is

$$\mu = \mu'\mu_1 \pm (1+\mu_1^2\mu'^2 - \mu_1^2 - \mu'^2)^{1/2}. \tag{29}$$

This equation yields different values for the step scattering limits of μ, for different values of the incident angle μ', which does not facilitate biasing, as we do not have a fixed value of the step scattering range of the phase function. Also, the azimuthal angle range is correspondingly different for different values of the incident direction cosine. The only way we can keep the polar direction cosine and the azimuthal angle range for the step scattering constant is to sample for the scattered direction cosine, υ, and the azimuthal angle of scattering, φ, with reference to the incident direction cosine μ', at every location, and use these to get the global physical direction cosine as [8]

$$\mu = \mu'\upsilon - (1-\mu'^2)^{1/2}(1-\upsilon^2)^{1/2}\cos\varphi. \tag{30}$$

If $\upsilon \leqslant \mu_1$, the step scattering holds for all φ, as illustrated in Fig. 5. We observe here that it is necessary to sample for φ, to obtain μ using equation (30), for every scatter. The method for the biasing of scatter in the step direction is outlined next.

We know from the CDF for isotropic scatter $[F(\theta) = (1-\mu)/2]$ that the probability of scatter in the step range is

$$P\{\mu_1 < \mu < 1\} = (1-\mu_1)/2. \tag{31}$$

Now, if we want this probability as Υ, the steps to be taken are:

(1) Sample ξ from a uniform distribution.

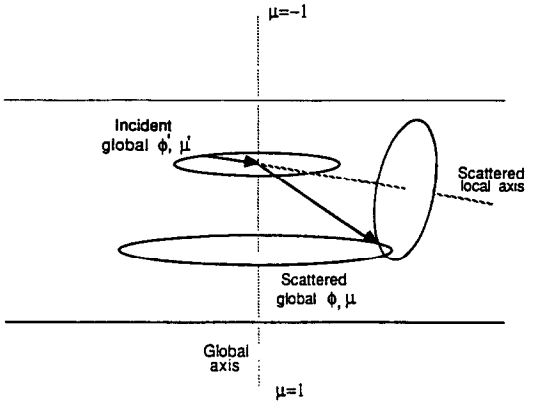

FIG. 5. Sampling for scattered direction from incident axis and global axis.

(2) If $\xi < \Upsilon$, assume scattering takes place in the forward peak and use the step value times ω as the unknown importance sampling weight. Else, assume scattering in the isotropic range and use the corresponding weight.

(3) Calculate the multiplicative biasing weight for the scatter as

$$W_b = \begin{cases} (1-\mu_1)/2\Upsilon & \text{forward step scattering} \\ (1+\mu_1)/2\Upsilon & \text{isotropic scattering.} \end{cases} \tag{32}$$

This is just the ratio of the actual probability given by equation (31), to the assumed value.

(4) Get the local direction cosine of the scattering angle, υ, as

$$\upsilon = \begin{cases} \dfrac{\xi}{\Upsilon}(1-\mu_1)+\mu_1 & \text{forward step scattering} \\ \dfrac{\xi-1}{\Upsilon-1}(1+\mu_1)-1 & \text{isotropic scattering} \end{cases} \tag{33}$$

within the respective ranges for step or isotropic scattering, using the generated random number.

(5) Sample the azimuthal angle φ, from equation (28) with $\varphi = \phi$, using a different random number.

(6) Calculate μ from equation (30).

For every scatter, the history weight is multiplied by the weight W_b. Last flight estimation is then employed to score for the backscattered or transmitted flux. The coefficients form an array of two dimensions, which are scored depending on whether scattering takes place within or outside the step range.

One of the unknowns to be evaluated is the single scattering albedo, ω. For the other unknown we choose

$$c = 1-h(1-\mu_1) \tag{34}$$

which is the second term on the right-hand side of equation (20) and its bounds are $(-1 < c < 1)$. The value of h in equation (20) can always be found, with a choice of μ_1, from equation (34).

We then obtain equations of the form

$$\hat{A}_k = \sum_{i=0}^{\nu} \sum_{l=0}^{\nu-i} b_{il,k}\omega^{i+l}c^l(c+2h)^l \qquad (35)$$

where

$$\hat{A}_k \equiv [1-Q(0)] \quad \text{or} \quad Q(1)$$

for the backscattered flux and transmission. Here $M = 2$ as we have two unknowns to evaluate, ν is the total number of scatters in the medium before escape or termination of the history, i the number of scatters in the isotropic range, l the number in the step range.

The coefficients b_{il} are obtained as

$$b_{il,k} = \frac{W_s}{N} \sum_{j=1}^{J} W_{\mathrm{f},j} \prod_{p=1}^{i+l} W_{\mathrm{b,p},l} \quad \text{for } k = 1, 2, \ldots, K \qquad (36)$$

where $J = J_0$ or J_1 is the total number of histories in which $\mu_l > 0$ or $\mu_l < 0$, respectively, for the $(i+l)$th scatter, τ_0 the total optical thickness, τ_l the optical thickness at which the scatter occurs. Thus, we have two equations for the backscattered flux and transmission, which we can solve for the two unknowns ω and c, using a least squares minimization technique. It should be noted that the coefficients b_{il} can be used with several sets of experimental observations for the same set of unknowns, without having to solve the direct problem again. Also, if the values of τ_0 and W_s are the same, the coefficients b_{il} can be used with the observed values of fluxes for different media with different ω or c.

Inverse solution for single homogeneous layer

In this section, we discuss the inverse Monte Carlo results obtained for a single, homogeneous, anisotropically scattering layer. The results from the F_9 method of solution [47] of the direct problem were used as the input to the inverse problem. Two different phase functions were considered: one for a pulverized-coal size distribution and the other for a monosize particle cloud. The phase function for the coal size distribution was obtained by evaluating the phase function for 10 monosize particles, multiplying their coefficients by a constant weight 0.1, and adding the coefficients of the same order. The first phase function (PF-I) has 19 terms in the Legendre expansion, and the other (PF-II) has 6 terms. In Fig. 6, the first phase function and its step function approximations are shown. The corresponding Legendre polynomial coefficients and other details are discussed in ref. [37].

The direct Monte Carlo results were obtained by using the SI approximation, with $\tau_0 = 1$, $\omega = 0.5, 0.8$, and 50 000 histories, 10 scatters, and were accurate for all values of μ_1 as compared to the F_9 results. These results are given in Tables 2 and 3 for both phase functions.

In actual experiments, the exit fluxes $Q(0)$ and $Q(\tau_0)$ are usually measured. Here, we present inverse results obtained from these quantities. For PF-I, we considered errors within $\pm 10\%$ for $Q(0)$, and $\pm 5\%$ for $Q(1)$. Since $Q(0)$ is typically an order of magnitude smaller than $Q(1)$, it is more likely to have a larger

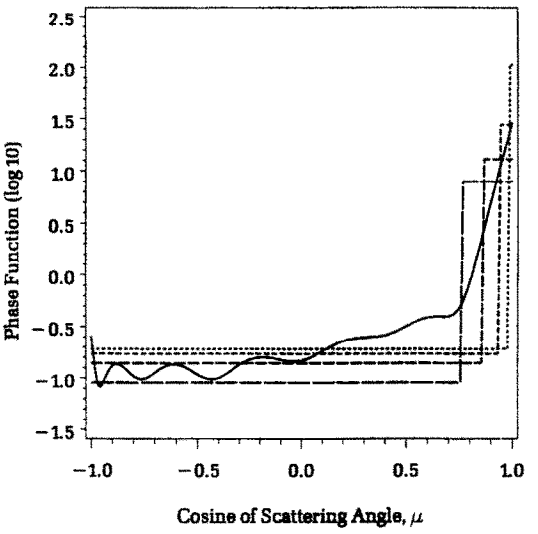

FIG. 6. Phase function for pulverized-coal size distribution. Exact results (solid line) from Lorenz–Mie theory (19 terms). Step approximations with 10, 20, 30, and 40 deg for the forward step.

percentage error. For PF-II, however, fluxes are of the same magnitude and we take errors within $\pm 5\%$ for both $Q(0)$ and $Q(1)$. In Figs. 7 and 8 we plotted the inverse solution results for different random errors in the observations. For these computations, a fixed value of $\Delta\Theta_1 = 10$ deg was used. The upper bounds were calculated with the maximum error using equation (14), and $r = 0.25$. The error estimates using equation (14) are indicative of the maximum possible errors in the inverted results. We note that equation (14) yields the upper bounds for the errors in $\hat{c}$, since this is the unknown in the least squares routine, and we multiply this quantity by $1.5(1+\mu_1)$ to obtain the upper bounds for the errors in $\hat{a}_1$.

The values of $\hat{\omega}$ obtained were very close to the actual values for all the cases considered in Figs. 7 and 8 (as well as others reported in ref. [37]). With other error bounds on the observations, the scatter in the recovered $\hat{a}_1$ was found to be more when $\omega = 0.5$ than when $\omega = 0.8$ [37]. From this we can conclude that better inverse results can be obtained for a_1 with larger ω values. Also, since the absolute errors in a_1 are the same for different phase functions when ω is a constant, we conclude that better inverse results are possible for larger values of a_1, i.e. for highly forward scattering phase functions. This is not surprising because of the choice of the phase function approximation. We also notice that the average of the 20 inverse results are close to those computed without errors in the observations. This means that, if the mean of several experimental observations is close to the exact value, the mean of the inverse results will also be close to their actual value, depending on the accuracy of the direct method.

Next the effect of τ_0 on the inverse results was considered. Two different values of optical thicknesses,

Table 2. Direct and inverse Monte Carlo results. With step-isotropic approximation for 19 term phase function. Direct F_N results $[1-Q(0)] = 0.96818$, $Q(1) = 0.40608$, $\omega = 0.5$, $a_1 = 2.4094$, $\tau_0 = 1$, $n = 10$, $N = 50\,000$

		Direct results		Inverse results		
$\Delta\theta$	Seed	$1-Q(0)$	$Q(1)$	ω	a_1	NI
10	I	0.9682	0.4111	0.492	2.394	20
	II	0.9672	0.4197	0.494	2.383	20
20	I	0.9687	0.4046	0.495	2.405	19
	II	0.9690	0.4061	0.496	2.395	19
30	I	0.9681	0.4051	0.497	2.414	18
	II	0.9682	0.4033	0.500	2.419	19
40	I	0.9678	0.4050	0.498	2.420	12
	II	0.9678	0.4044	0.502	2.421	12
50	I	0.9688	0.4038	0.503	2.408	16
	II	0.9675	0.4041	0.504	2.428	19

NI, Number of iterations.
I, Seed 34 567.
II, Seed 76 543.

$\tau_0 = 0.1$ and 2.0 were used with the phase function 1. In the direct Monte Carlo method 20 scatters and 50 000 histories were employed. The random errors were equal to those considered before. A large number of histories were required for acceptable direct results for small optical thicknesses. In general, accuracy of the inversion was better at large optical thickness. This was because there were fewer scatters within the medium when τ is small.

CONCLUSIONS

In this paper, we presented a methodology for solution of the inverse radiation problem using a Monte Carlo technique. This method can be used to determine a functional variation of single scattering albedo in an inhomogeneous medium, and the single scattering albedo and the asymmetry factor in a homogeneous, anisotropically scattering slab.

The method was shown to be capable of accounting for the anisotropic scattering phase function in the medium if radiation intensity distribution was available from the experiments. It is preferable to use a step-isotropic (SI) phase function approximation in the inverse analysis, because it is sufficiently accurate for highly-forward scattering particles. The use of the step-Eddington (SE) approximation in the inverse method requires one additional variable to be determined—the second coefficient of the scattering phase function. The direct and inverse solution, however, become more involved and cumbersome, and the accuracy of inverse calculations are no better than those using the SI approximation.

One limitation in the present Monte Carlo inverse method is that τ_0 is to be known a priori for the solution, i.e. that β is to be known. If β is also to be evaluated, we must perform several direct simulations, which eliminates the most important advantage of the Monte Carlo method as used so far. However, since the direct simulation will use specific values of the

Table 3. Direct and inverse Monte Carlo results. With step-isotropic approximation for six term phase function. Direct F_N results $[1-Q(0)] = 0.76057$, $Q(1) = 0.45588$, $\omega = 0.8$, $a_1 = 0.6438$, $\tau_0 = 1$, $n = 10$, $N = 50\,000$

		Direct results		Inverse results		
$\Delta\theta$	Seed	$1-Q(0)$	$Q(1)$	ω	a_1	NI
10	I	0.7631	0.4572	0.801	0.616	21
	II	0.7692	0.4553	0.807	0.585	21
20	I	0.7605	0.4569	0.800	0.637	22
	II	0.7629	0.4602	0.805	0.596	21
30	I	0.7607	0.4564	0.800	0.639	22
	II	0.7630	0.4588	0.805	0.604	21
40	I	0.7600	0.4566	0.799	0.642	22
	II	0.7622	0.4582	0.805	0.614	21
50	I	0.7604	0.4561	0.799	0.643	22
	II	0.7619	0.4583	0.804	0.615	22
60	I	0.7603	0.4558	0.798	0.646	22
	II	0.7615	0.4588	0.802	0.615	22

NI, Number of iterations.
I, Seed 34 567.
II, Seed 76 543.

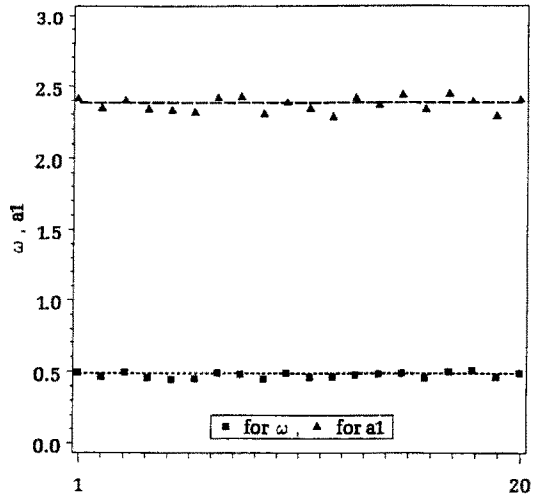

FIG. 7. Inverse results for the single scattering albedo and the first coefficient of the phase function expansion, and the mean values. The exact values are $\tau_0 = 1.0$, $\omega = 0.5$, and $a_1 = 2.409$ (PF-1). Random errors are within $\pm 10\%$ for $Q(0)$ and $\pm 5\%$ for $Q(1)$. Converged values without error are $\omega = 0.492$ and $a_1 = 2.394$. The upper bounds are ± 0.040 for $\hat{\omega}$ and ± 0.453 for $\hat{a}_1$.

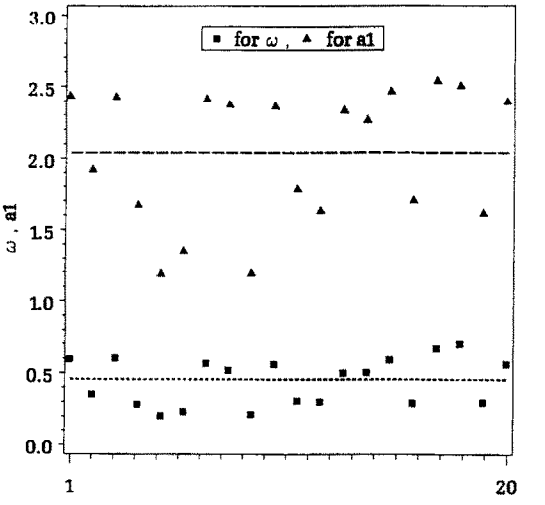

FIG. 9. Inverse results for the single scattering albedo and the first coefficient of the phase function expansion, and the mean values. The exact values are $\tau_0 = 0.1$, $\omega = 0.5$, and $a_1 = 2.409$ (PF-1). Random errors are within $\pm 10\%$ for $Q(0)$ and $\pm 5\%$ for $Q(1)$. Converged values without error are $\omega = 0.497$ and $a_1 = 2.278$. The upper bounds are ± 0.389 for $\hat{\omega}$ and ± 8.252 for $\hat{a}_1$.

unknowns for use in the least squares routine, we need not use importance sampling or evaluate and store the coefficients b_{il}. This will lead to a reduction in the computational time for each direct run.

The Monte Carlo solution algorithm developed in this work can be extended to multidimensional rectangular and cylindrical geometries readily. However, because the problem becomes three-dimensional, the computational time required for the solution may increase significantly.

Acknowledgements—This research is supported by the Department of Energy Grant No. DE-FG22-87PC79916 and the National Science Foundation Grant No. CBT-8708679.

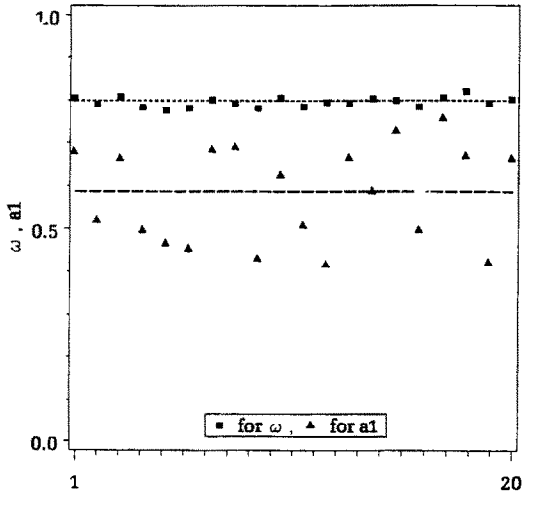

FIG. 8. Inverse results for the single scattering albedo and the first coefficient of the phase function expansion, and the mean values. The exact values are $\tau_0 = 1.0$, $\omega = 0.8$, and $a_1 = 0.644$ (PF-2). Random errors are within $\pm 5\%$ for $Q(0)$ and $\pm 5\%$ for $Q(1)$. Converged values without error are $\omega = 0.801$ and $a_1 = 0.616$. The upper bounds are ± 0.027 for $\hat{\omega}$ and ± 0.246 for $\hat{a}_1$.

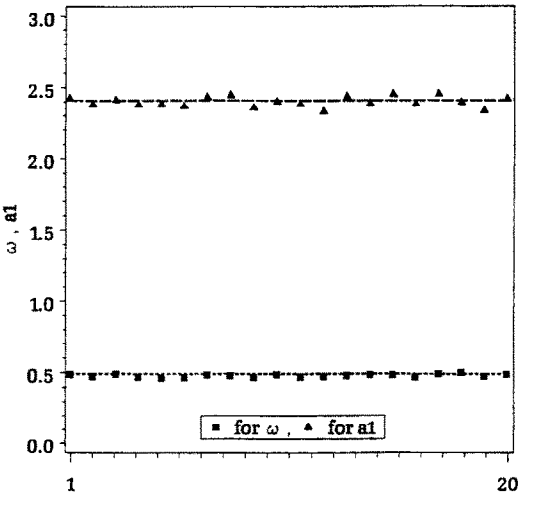

FIG. 10. Inverse results for the single scattering albedo and the first coefficient of the phase function expansion, and the mean values. The exact values are $\tau_0 = 2.0$, $\omega = 0.5$, and $a_1 = 2.409$ (PF-1). Random errors are within $\pm 10\%$ for $Q(0)$ and $\pm 5\%$ for $Q(1)$. Converged values without error are $\omega_0 = 0.493$ and $a_1 = 2.420$. The upper bounds are ± 0.017 for $\hat{\omega}$ and ± 0.169 for $\hat{a}_1$.

Support for S. Subramaniam from the Center for Computational Sciences at the University of Kentucky is also gratefully acknowledged.

REFERENCES

1. R. Viskanta and M. P. Mengüç, Radiation transfer in combustion systems, *Prog. Energy Combust. Sci.* **13,** 97–160 (1987).
2. R. Siegel and J. R. Howell, *Thermal Radiation Heat Transfer*. Hemisphere, New York (1981).
3. M. N. Özişik, *Radiative Transfer and Interactions with Conduction and Convection*. Wiley, New York (1973).
4. R. Viskanta, Radiative heat transfer, *Prog. Chem. Engng* **22,** 51–81 (1984).
5. E. E. Lewis and W. F. Miller, Jr., *Computational Methods of Neutron Transport*. Wiley, New York (1984).
6. J. R. Howell, Thermal radiation in participating media: the past, the present, and some possible futures, *J. Heat Transfer* **110,** 1220–1229 (1988).
7. H. Kahn, Random sampling (Monte Carlo) techniques in neutron attenuation problems, *Nucleonics* **6,** 27–33, 36, 60–65 (1950).
8. N. M. Schaeffer, Reactor shielding for nuclear engineers, U.S. Atomic Energy Commission, TID-25951 (1973).
9. E. J. McGrath and D. C. Irving, Techniques for efficient Monte Carlo simulation, ORNL-RSIC-38, Vol. III (1975).
10. C. E. Siewert, A new approach to the inverse problem, *J. Math. Phys.* **19,** 2619–2621 (1978).
11. W. L. Dunn, Inverse Monte Carlo analysis, *J. Comput. Phys.* **41,** 154–166 (1981).
12. C.-H. Ho and M. N. Özişik, An inverse radiation problem, *Int. J. Heat Mass Transfer* **32,** 335–341 (1989).
13. C. E. Siewert, On establishing a two term scattering law in the theory of radiative transfer, *J. Appl. Math. Phys.* **30,** 517–525 (1979).
14. C. E. Siewert, On the inverse problem for a three term phase function, *J. Quant. Spectrosc. Radiat. Transfer* **22,** 441–446 (1979).
15. N. J. McCormick, Transport scattering coefficients from reflection and transmission measurements, *J. Math. Phys.* **20,** 1504–1507 (1979).
16. W. L. Dunn and J. L. Maiorino, On the numerical characteristics of an inverse solution for three term radiative transfer, *J. Quant. Spectrosc. Radiat. Transfer* **24,** 203–209 (1980).
17. N. J. McCormick and R. Sanchez, Inverse problem transport calculations for anisotropic scattering coefficients, *J. Math. Phys.* **22,** 199–208 (1981).
18. N. J. McCormick, Inverse methods for determination of properties of optically thick atmospheres, *Appl. Optics* **22**(17), 2556–2558 (1983).
19. S. Karanjai and M. Karanjai, Inverse radiative problem with delta-Eddington phase function in a symmetric model, *Astrophys. Space Sci.* **117,** 151–164 (1985).
20. S. Karanjai and M. Karanjai, Inverse radiative problem with delta-Eddington phase function in a nonsymmetric model, *Astrophys. Space Sci.* **117,** 387–400 (1985).
21. S. J. Wilson and K. K. Sen, Moment method for the inverse radiative transfer in inhomogeneous media, *Astrophys. Space J.* **119,** 93–96 (1986).
22. N. J. McCormick, Inverse radiative transfer with a delta-Eddington phase function, *Astrophys. Space Sci.* **129,** 331–334 (1987).
23. K. Kamiuto and J. Seki, Study of the P_1 approximation in an inverse scattering problem, *J. Quant. Spectrosc. Radiat. Transfer* **37,** 455–459 (1987).
24. K. Kamiuto, A constrained least squares method for limited inverse scattering problems, *J. Quant. Spectrosc. Radiat. Transfer* **40,** 47–50 (1988).
25. W. L. Dunn, Inverse Monte Carlo solutions for radiative transfer in inhomogeneous media, *J. Quant. Spectrosc. Radiat. Transfer* **29,** 19–26 (1983).
26. C.-H. Ho and M. N. Özişik, Inverse radiation problems in inhomogeneous media. *J. Quant. Spectrosc. Radiat. Transfer* **40,** 553–560 (1988).
27. I. N. Mel'nikova, The field of scattered solar radiation in a cloud layer, *Izv. Atmos. Ocean Phys.* **14,** 928–931 (1978).
28. M. D. King, A method for determining the single-scattering albedo of clouds through observations of the infrared scattered radiation field, *J. Atmos. Sci.* **38,** 2031–2044 (1981).
29. N. J. McCormick, Methods for estimating the similarity parameter of clouds from internal measurements of the scattered radiation field, *J. Quant. Spectrosc. Radiat. Transfer* **33,** 63–70 (1985).
30. T. Duracz and N. J. McCormick, Equations for estimating the similarity parameter for radiation measurements within weakly absorbing optically thick clouds, *J. Atmos. Sci.* **43,** 486–492 (1986).
31. N. J. McCormick, A critique of inverse solutions to slab geometry transport problems, *Prog. Nucl. Energy* **8,** 235–245 (1981).
32. N. J. McCormick, Recent developments in inverse scattering transport methods, *Transport Theory Statist. Phys.* **13,** 15–28 (1984).
33. N. J. McCormick, Methods for solving inverse problems for radiation transport—an update, *Transport Theory Statist. Phys.* **15,** 759–772 (1986).
34. M. Kanal and J. A. Davies, A multidimensional inverse problem in transport theory, *Transport Theory Statist. Phys.* **8,** 99–115 (1979).
35. E. W. Larsen, Solution of multidimensional inverse transport problems, *J. Math. Phys.* **25,** 131–135 (1984).
36. E. W. Larsen, Solution of three dimensional inverse transport problems, *Transport Theory Statist. Phys.* **17,** 147–167 (1988).
37. S. Subramaniam, Solution of the inverse radiation problem using a Monte Carlo technique, M.S. Thesis, University of Kentucky, Lexington, Kentucky (1989).
38. S. Subramaniam and M. P. Mengüç, Inverse radiation problem in single and double layer planar systems with a Monte Carlo technique, *Proc. AIAA–ASME Joint Thermophys. and Heat Transfer Conf.*, Seattle, Washington, July, HTD-Vol. 137 (1990).
39. *IMSL Library*, Edn 10, NBC Building, 7500 Ballaire Blvd., Houston, TX 77036-5085, U.S.A. (1987).
40. J. E. Dennis, Jr. and R. B. Schnabel, *Numerical Methods for Unconstrained Optimization and Nonlinear Equations*. Prentice-Hall, Englewood Cliffs, New Jersey (1983).
41. P. E. Gill and W. Murray, Minimization subject to bounds on the variables, NPL Report NAC72, National Physical Laboratory, U.K. (1976).
42. A. R. Gallant, *Nonlinear Statistical Models*, Wiley Series in Probability and Mathematical Statistics. Wiley, New York (1987).
43. R. D. M. Garcia and C. E. Siewert, Radiative transfer in finite inhomogeneous plane-parallel atmospheres, *J. Quant. Spectrosc. Radiat. Transfer* **27,** 141–148 (1982).
44. K. Stamnes, S. C. Tsay, W. Wiscombe and K. Jayaweera, A numerically stable algorithm for discrete-ordinate-method radiative transfer in multiple scattering and emitting layered media, *Appl. Optics* **27,** 2502–2509 (1988).
45. M. P. Mengüç and S. Subramaniam, Step phase function approximation, *J. Quant. Spectrosc. Radiat. Transfer* **43,** 253–265 (1990).
46. G. C. Pomraning, On the Henyey–Greenstein approximation to scattering phase functions, *J. Quant. Spectrosc. Radiat. Transfer* **39,** 109–113 (1988).
47. M. P. Mengüç and R. Viskanta, Comparison of radiative transfer approximations for a highly forward scattering planar medium, *J. Quant. Spectrosc. Radiat. Transfer* **29,** 381–394 (1983).

SOLUTION PAR LA TECHNIQUE MONTE CARLO DU PROBLEME INVERSE DE RAYONNEMENT POUR UN MILIEU NON HOMOGENE ET A DIFFUSION ANISOTROPE

Résumé—On présente une analyse de résolution du problème inverse de rayonnement par une technique Monte Carlo. Pour un milieu planaire non homogène, le profil de l'albedo est obtenu par l'analyse inverse. Pour des milieux homogènes, diffusant anisotropiquement, l'albedo et le facteur d'asymétrie se recouvrent. On utilise une approximation pour fonction échelon pour tenir compte de la diffusion anisotrope dans le milieu. Les limites de confiance dans l'estimation des paramètres sont évaluées. Les résultats montrent que les propriétés du milieu peuvent être retrouvées avec une grande précision même s'il y a 10% d'erreur dans les données d'entrée. Le principal avantage de la méthode Monte Carlo est qu'une solution unique directe fournit les coefficients d'un polynôme à multivariable pour chaque ensemble de données, qui sont ensuite utilisés pour obtenir les propriétés du milieu par une technique non linéaire de minimisation par moindres carrés.

LÖSUNG DES INVERSEN STRAHLUNGSPROBLEMS FÜR INHOMOGENE UND ANISOTROP STREUENDE MEDIEN MIT HILFE DER MONTE-CARLO-METHODE

Zusammenfassung—Für die Lösung des inversen Strahlungsproblems wird unter Verwendung der Monte-Carlo-Méthode ein Ansatz vorgestellt. Die inverse Berechnung ergibt für inhomogene ebene Medien das Profil des Albedo durch Einfachstrahlung. Für homogene, anisotrop streuende Medien werden das Einfach-Streuungsalbedo und der Asymmetrie-Faktor angegeben. Die anisotrope Streuung in Medien wird mit Hilfe einer Sprungfunktion angenähert. Fehler in den Eingabedaten verursachen eine bestimmte Unsicherheit bei den berechneten Parametern—deren Vertrauensgrenzen werden berechnet. Die Ergebnisse zeigen, daß die Eigenschaften des Mediums mit hoher Genauigkeit ermittelt werden können, sogar im Falle eines zehnprozentigen Fehlers bei den Eingabedaten. Der Hauptvorteil des Monte-Carlo-Verfahrens ist, daß eine einzige direkte Lösung die Koeffizienten eines Polynoms mit mehreren Variablen für jeden Datensatz hervorbringt. Diese werden dann benutzt, um mit Hilfe der Nichtlinearen Regression die Eigenschaften des Mediums zu berechnen.

РЕШЕНИЕ ОБРАТНОЙ ЗАДАЧИ ИЗЛУЧЕНИЯ ДЛЯ НЕОДНОРОДНЫХ И АНИЗОТРОПНО РАССЕИВАЮЩИХ СРЕД МЕТОДОМ МОНТЕ КАРЛО

Аннотация—Проведен анализ решения обратной задачи излучения методом Монте Карло. С помощью обратного анализа получен профиль единичного альбедо рассеяния для неоднородных плоских сред. Для однородных, анизотропно рассеивающих сред определены единичный альбедо рассеяния и коэффициент асимметрии. С целью учета анизотропного рассеяния среды используется приближение ступенчатой фазовой функции. Получена оценка границы достоверности определения параметров при различных погрешностях во входных данных. Результаты показывают, что свойства среды могут быть определены с высокой точностью даже при 10%-ной погрешности во входных данных. Основное преимущество метода Монте Карло состоит в том, что единичное прямое решение позволяет получить коэффициенты полинома со многими переменными для каждой серии экспериментальных данных, которые затем используются для определения свойств среды нелинейным методом минимизации наименьших квадратов.